23rd International Conference
ENGINEERING MECHANICS 2017
Svratka, Czech Republic, 15 – 18 May 2017

THREE-POINT BENDING FATIGUE DAMAGE MECHANISMS ASSOCIATED WITH THE DIFFERENT STRUCTURE OF AL-MG CAST ALLOYS

M. Uhríčik*, M. Oravcová*, P. Palček*, M. Chalupová*, L. Kucharikova*

Abstract: *The article is monitoring the influence of the structure on the fatigue properties of aluminium alloys for the casting of type Al-Mg. As an experimental material were used aluminium alloys EN AC 51200 and EN AC 51500, supplied in a cast state without a heat treatment. These alloys were selected on the basis of the chemical composition, where the content of most alloying elements is comparable, only in the case of the concentration of magnesium are these alloys significantly different. Fatigue properties of aluminium alloys were tested by three-point bending cyclic loading. The fracture surface of the testing sample was examined using scanning electron microscopy (SEM), where samples were observed on various stages of the fatigue process, their characteristics and differences of fracture surfaces.*

Keywords: Fatigue, Fracture, Aluminium alloy, Three-point bending loading, Structure.

1. Introduction

Fatigue failures in metallic structures are a well-known technical problem. In a specimen subjected to a cyclic load, a fatigue crack nucleus can be initiated on a microscopically small scale, followed by crack grows to a macroscopic size, and finally to specimen failure in the last cycle of the fatigue life. Understanding of the fatigue mechanism is essential for considering various technical conditions which affect fatigue life and fatigue crack growth, such as the material surface quality, residual stress, and environmental influence. This knowledge is essential for the analysis of fatigue properties of an engineering structure (Belan et al., 2014 and Hurtalová et al., 2014).

2. Material characteristics

As an experimental material were used aluminium cast alloys of type Al-Mg (EN AC-51200 and EN AC-51500), supplied in a cast state without a heat treatment in the form of plates. They were produced by the continuous casting method. Test samples for determining the fatigue properties were made by the cutting operation from these plates, which were cut from casts. The chemical composition of both alloys was examined by spark emission spectrometer SPECTROMAXx and results are shown in Tab. 1. These alloys were selected based on this chemical composition, where the content of most of alloying elements is comparable, only a concentration of magnesium is considerably different.

3. Results and discusion

3.1. Microstructural analysis and phase analysis

Considering that alloys were casted under the same technological conditions, it can be said that the structure affects only the chemical composition of alloys. Microstructure of materials is expressively dendritic (Fig. 1 and Fig. 2). The highest percentage representation of dendrites has α-phase (matrix) that is a solid solution of aluminium together with other additive elements. In the structure, there is also an

* Ing. Milan Uhríčik, PhD., Ing. Monika Oravcová, Prof. Ing. Peter Palček, PhD., Ing. Mária Chalupová, Ing. Lenka Kucharikova, PhD. : Department of Materials Engineering, University of Žilina, Univerzitná 8215/1; 010 26, Žilina; SK, milan.uhricik@fstroj.uniza.sk, monika.oravcova@fstroj.uniza.sk, peter.palcek@fstroj.uniza.sk, maria.chalupova@fstroj.uniza.sk, lenka.kucharikova@fstroj.uniza.sk

intermetallic phase Mg_2Si. This phase has a different morphology in alloys. In the case of EN AC 51200 alloy, it has a shape of skeleton formation and is distributed in interdendritic areas. There is also β-phase, which is formed in interdendritic areas and has a stoichiometric basis Al_3Mg_2. In alloy EN AC 51500, intermetallic phase Mg_2Si has a finer morphology and does not have a typical shape of skeleton formation. Because elements such as iron and manganese are also in alloys, can be observed a small amount of Fe-rich phase in structure of both materials, probably $Al_6(FeMn)$. β-phase is not present in this alloy, because of the smaller content of magnesium.

Tab. 1: The chemical composition of alloys, in wt. %.

	Si	**Fe**	**Cu**	**Mn**	**Mg**	**Cr**	**Pb**	**Al**
EN AC 51200	1.3	0.102	0.003	0.416	10.32	0.006	0.027	balance
EN AC 51500	1.53	0.11	0.004	0.529	6.28	0.008	0.031	balance

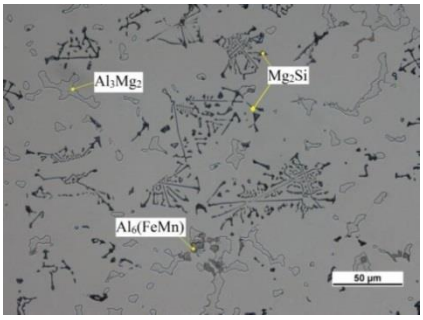

Fig. 1: Microstructures of allos EN AC 51200.

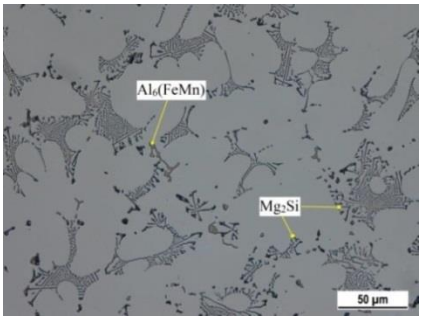

Fig. 2: Microstructures of alloy EN AC 51500.

3.2. Fatigue lifetime

Fatigue tests were carried out on the test equipment ZWICK/ROELL AMSLER 150 HFP 5100 according to norm STN 42 0363. This equipment is using the resonance principle with constant or variable amplitude and mean load. Smooth rectangular specimens without notches (10 x 18 x 40 mm) were loaded by cyclic three-point bending loading with mean stress σ_m = -144 MPa and frequency 120 Hz, only stress amplitude was changing. From results of fatigue tests were constructed graphs σ_a-N in semi-logarithmic coordinates, for every alloy (Fig. 3 and Fig. 4). By comparing of graphs can be stated that alloy EN AC 51500 has better fatigue properties than alloy EN AC 51200 in analyzed area of the number of cycles.

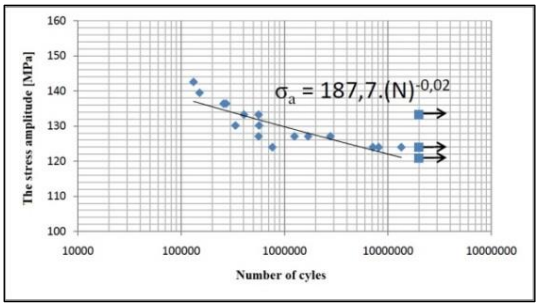

Fig. 3: Results of fatigue tests for alloy EN AC 51200.

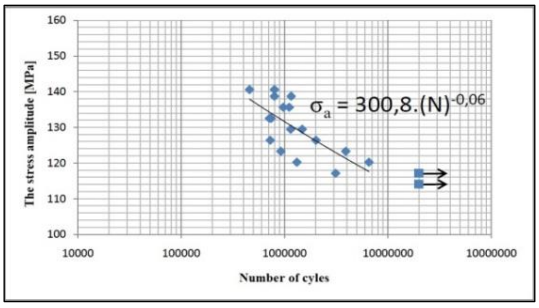

Fig. 4 Results of fatigue tests for alloy EN AC 51500.

3.3. Fractographic analysis

Fractographical assessment of fracture surfaces was realized on samples from each material after the fatigue test. On samples were observed various stages of fatigue process, their characteristics and differences of fracture surfaces between samples loading in high and low amplitude of stress. It has also been observed an area of final fracture. Fracture surfaces were evaluated by scanning electron microscopy TESCAN VEGA LMU II. From analysis it is possible to determine initiation (nucleation) of fatigue crack, surfaces of individual areas of fracture, namely the fatigue fracture area and the area of static final failure.

A general view of the fracture area for the alloy EN AC 51500 after 1314148 cycles at a stress of 120 MPa it documented in Fig. 5a, where can be seen various stages of fatigue process. Detail of initiation site is shown in Fig. 5b. Transgranular fatigue failure of α-phase (matrix) and there were observed typical signs of fatigue – striations and also an interfacial and a fission failure of Mg_2Si phase, this all is shown in Fig. 5c. Fig. 5d displays the area of static final failure, where can be seen plastic´s transformed ridges of α-phase, together with a transgranular ductile fracture of α-phase with dimple morphology and also is visible an interfacial failure of Mg_2Si phase.

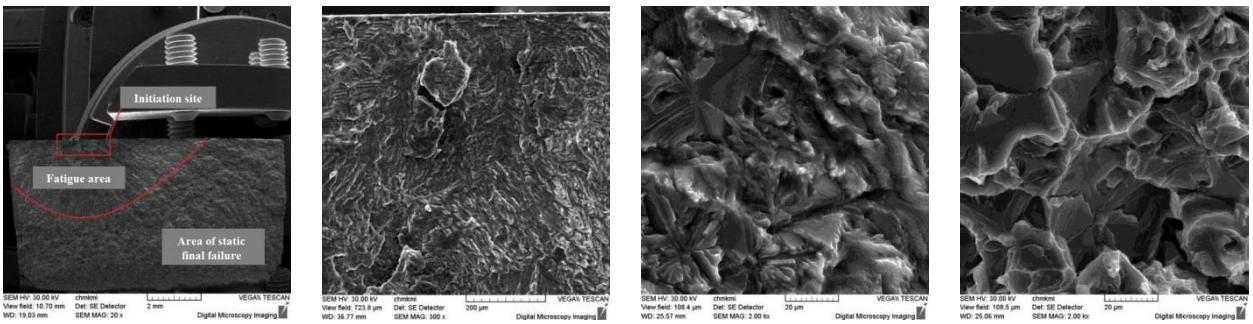

a) a general view. *b) a detail of initiation site.* *c) a detail from the fatigue area.* *d) a detail from the area of static final failure.*

Fig. 5: Fracture surface of aluminium alloy 51500, σ_a = 120 MPa, N_f = 1314148 cycles.

A general view of the fracture area for the alloy EN AC 51500 after 799229 cycles at a stress of 138 MPa is shown in Fig. 6a. Here can be seen that when higher amplitude of stress was applicate, the fatigue crack was spread from several initiation sites on the specimen surface and there was also a reduction of the fatigue area. Detail of one initiation site is shown in Fig. 6b. Transgranular fatigue failure of α-phase (matrix) and there were observed typical signs of fatigue – striations a it is shown in Fig 6c. Fig. 6d displays the area of static final failure, where can be also seen plastic´s transformed ridges of α-phase, together with transgranular ductile fracture of α-phase with dimple morphology and also is visible an interfacial failure of Mg_2Si phase.

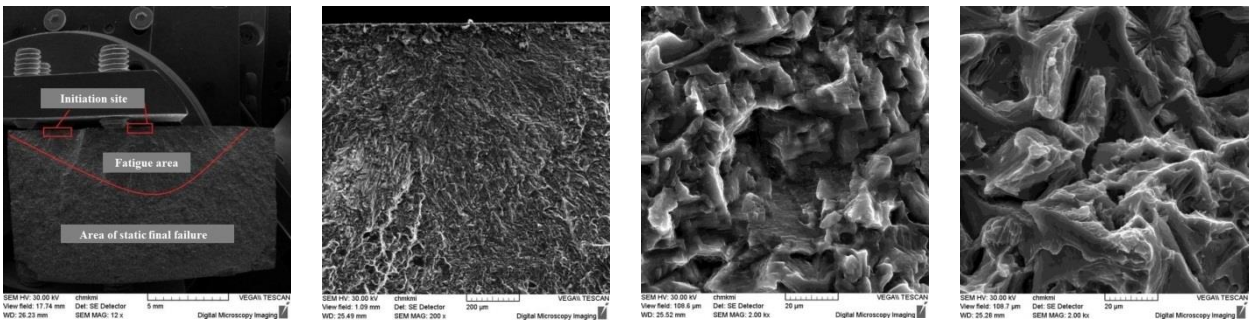

a) a general view. *b) a detail of initiation site.* *c) a detail from the fatigue area.* *d) a detail from the area of static final failure.*

Fig. 6: Fracture surface of aluminium alloy 51500, σ_a = 138 MPa, N_f = 799229 cycles.

A general view of the fracture area for the alloy EN AC 51200 after 761899 cycles at a stress of 124 MPa is documented in Fig. 7a, where can be seen various stages of fatigue process. Detail of initiation site is shown in Fig. 7b. In Fig 7c can be seen an interfacial failure of intermetallic phases (Al_3Mg_2, $Al_6(FeMn)$ and Mg_2Si) and also a transgranular fatigue failure of α-phase (matrix). Fig. 7d displays the area of static final failure, where can be seen interfacially broken intermetallic phases and plastic´s transformed ridges of α-phase, together with transgranular ductile fracture of α-phase with dimple morphology.

A general view of the fracture area for the alloy EN AC 51200 after 150530 cycles at a stress of 139 MPa is shown in Fig. 8a. Here can be seen that when higher amplitude of stress was applicate, the fatigue crack was spread from several initiation sites on the specimen surface and there was also a reduction of the fatigue area and a smaller number of cycles to fracture. Detail of one initiation site is shown in Fig. 8b. In Fig 8c can be seen a transgranular fatigue failure of α-phase (matrix) and also an interfacial failure of intermetallic phases (Al_3Mg_2 and $Al_6(FeMn)$). Fig. 8d displays the area of static final failure, where can be seen plastic´s transformed ridges of α-phase, together with a transgranular ductile fracture of α-phase with dimple morphology and also is visible an interfacial failure of Mg_2Si and Al_3Mg_2 phases.

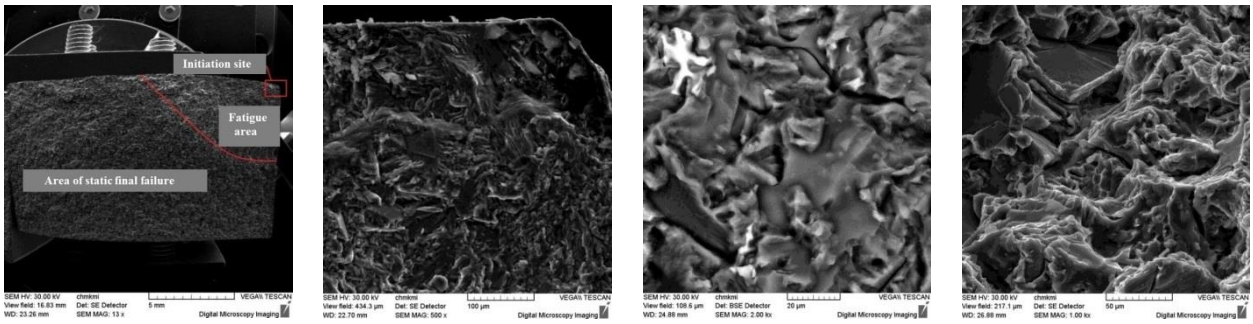

a) a general view. *b) a detail of initiation. site* *c) a detail from the. fatigue area* *d) a detail from the area. of static final failure*

Fig. 7: Fracture surface of aluminium alloy 51200, σ_a = 124 MPa, N_f = 761899 cycles.

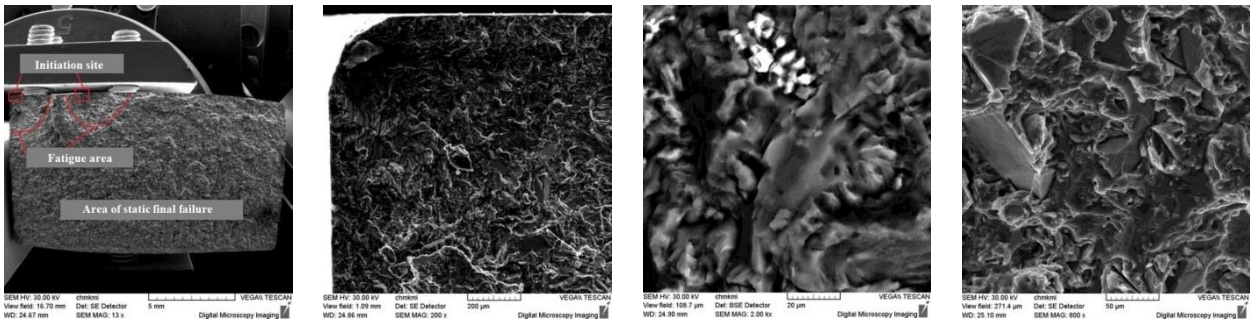

a) a general view. *b) a detail of initiation site.* *c) a detail from the fatigue area.* *d) a detail from the area of static final failure.*

Fig. 8: Fracture surface of aluminium alloy 51200, σ_a = 139 MPa, N_f = 150530 cycles.

4. Conclusions

Alloys have a clearly dendritic structure consisting mainly α-phase. In the structure of both alloys are intermetallic $Al_6(FeMn)$ and Mg_2Si phases. In alloy EN AC 51200, there is also an intermetallic Al_3Mg_2 phase. Alloys are comparable in terms of morphology and the amount of $Al_6(FeMn)$ phase. From fatigue tests, it can conclude that alloy EN AC 51500 has better fatigue properties than alloy EN AC 51200, in the analyzed areas of number of cycles under the same conditions of loading. Fraktographic analysis did not reveal significant changes of micromechanisms of fracture surfaces after fatigue tests. Fatigue area is characterized by transgranular fatigue failure of α-phase (matrix). Intermetallic phases in this area were violated interfacially, only Mg_2Si phase had also a fission failure somewhere. The area of static final failure is typical of a transgranular ductile fracture of α-phase with dimple morphology with plastic´s transformed ridges. When comparing both of alloys, it can be stated that the only difference is that on the fracture surface of alloy EN AC 51500 is not an interfacially broken Al_3Mg_2 phase, because this alloy does not contain it. In terms of stress amplitude can be said that in case of a higher amplitude of cyclic loading there was a multiple initiation of fatigue crack.

Acknowledgement

This work has been supported by Scientific Grant Agency of Ministry of Education of Slovak republic, N°1/0683/15 and N°1/0533/15.

References

Belan, J., Hurtalová, L., Vaško, A. and Tillová, E. (2014) Metallography evaluation of IN 718 after applied heat treatment. Manufacturing Technology, 14, 3, pp. 262-267.

Hurtalová, L., Tillová, E., Chalupová, M., Belan, J. and Vaško, A. (2014) Microstructure control of secondary A 231 cast alloy used in automotive industry. Manufacturing Technology, 14, 3, pp. 326-333.